Inhibition of Hsp90 activates osteoclast c-Src signaling and promotes growth of prostate carcinoma cells in bone

Akihiro Yano*, Shinji Tsutsumi*, Shiro Soga*†, Min-Jung Lee‡, Jane Trepel‡, Hiroyuki Osada§, and Len Neckers*¶

*Urologic Oncology Branch, Center for Cancer Research, National Cancer Institute, Building 10, Room 1-5940, Bethesda, MD 20892; ‡Medical Oncology Branch, National Cancer Institute, Bethesda, MD 20892; and §Antibiotics Laboratory, Discovery Research Institute, RIKEN, Saitama, 351-0198 Japan

Edited by Sue Hengren Wickner, National Institutes of Health, Bethesda, MD, and approved September 3, 2008 (received for review June 2, 2008)

Hsp90 inhibitors are being evaluated extensively in patients with advanced cancers. However, the impact of Hsp90 inhibition on signaling pathways in normal tissues and the effect that this may have on the antitumor activity of these molecularly targeted drugs have not been rigorously examined. Breast and prostate carcinomas are among those cancers that respond to Hsp90 inhibitors in animal xenograft models and in early studies in patients. Because these cancers frequently metastasize to bone, it is important to determine the impact of Hsp90 inhibitors in the bone environment. In the current study, we show that, in contrast to its activity against prostate cancer cells *in vitro* and its inhibition of s.c. prostate cancer xenografts, the Hsp90 inhibitor 17-AAG stimulates the intraosseous growth of PC-3M prostate carcinoma cells. This activity is mediated not by a direct effect on the tumor but by Hsp90-dependent stimulation of osteoclast maturation. Hsp90 inhibition transiently activates osteoclast Src kinase and promotes Src-dependent Akt activation. Both kinases are key drivers of osteoclast maturation, and three agents that block osteoclastogenesis, the Src inhibitor dasatinib, the bisphosphonate alendronate, and the osteoclast-specific apoptosis-inducer reveromycin A, markedly reduced 17-AAG-stimulated tumor growth in bone. These data emphasize the importance of understanding the complex role played by Hsp90 in regulating signal transduction pathways in normal tissues as well as in cancer cells, and they demonstrate that drug-dependent modulation of the local tumor environment may profoundly affect the antitumor efficacy of Hsp90-directed therapy.

cancer | geldanamycin | heat shock protein 90 | osteoclastogenesis

Heat shock protein (Hsp) 90 is a molecular chaperone required for the stability and function of multiple mutated, chimeric, and overexpressed signaling proteins that promote the growth and/or survival of cancer cells (1–3). Hsp90 inhibitors, by interacting with a single molecular target, cause the destabilization and eventual degradation of Hsp90 client proteins, including numerous kinases. Several chemically distinct Hsp90 inhibitors have shown promising anti-tumor activity *in vivo* (4–7), and one Hsp90 inhibitor, 17-AAG, is currently in late-stage clinical trial.

Recently, we demonstrated that Hsp90 interaction maintains the client protein c-Src in a metastable state, intermediate between active and inactive conformations (8). Disruption of Hsp90-c-Src association by exposure to 17-AAG results in transient Src kinase activation before Src destabilization and degradation. This phenomenon has also been observed for the RNA-dependent serine-threonine kinases PKR and Raf-1 (9, 10) and for the tyrosine kinase ErbB2 (11). Such transient activation, although short-lived itself, can in certain cases propagate a downstream signaling cascade of much longer duration (8).

Among solid tumors that have shown favorable preclinical and clinical responses to Hsp90 inhibitors are breast and prostate carcinomas (7, 12–17). Because these cancers have a propensity to metastasize to bone, it is important to determine the impact of Hsp90 inhibitors on tumor cells growing in this unique milieu. Although much emphasis has been placed on understanding the multifactorial effects of Hsp90 inhibition on cancer cell signaling networks, less attention has been given to the potential impact of inhibiting Hsp90 on the signaling processes of normal tissues, and to the unpredictable impact that this may have on tumor growth and survival in defined tissue environments.

In a study by Price *et al.* (18), 17-AAG was reported to promote formation of osteolytic lesions and bone metastases in a murine breast cancer model (18). Because Src kinase is essential for osteoclast maturation (19, 20), we examined the possibility that 17-AAG-induced Src activation in osteoclasts may mediate this phenomenon. Here, we report that Hsp90 inhibition promotes osteoclast maturation through Src kinase activation and strongly synergizes with the cytokines macrophage colony stimulating factor (M-CSF) and receptor activator of nuclear factor kappa B ligand (RANKL), two crucial drivers of this process (21, 22). As a result, and in direct contrast to its antitumor activity *in vitro* and in a s.c. xenograft model, 17-AAG indirectly stimulates the intraosseous growth of PC-3M prostate cancer cells. However, this can be counteracted by three mechanistically distinct inhibitors of osteoclastogenesis, a Src kinase inhibitor (23), a bisphosphonate (24), and the osteoclast-specific apoptosis inducer reveromycin A (25). This study emphasizes the importance of obtaining a more complete understanding of the complex role played by Hsp90 in regulating normal tissue homeostasis, and how these events impact tumor growth and response to targeted therapy.

Results

17-AAG Promotes Osteoclastogenesis Through Src Kinase Activation. The hypothesis of this study was that 17-AAG promotes osteoclastogenesis through Src kinase activation. To confirm this, we first examined whether 17-AAG activates Src in osteoclast progenitors. Using murine RAW 264.7 preosteoclast cells, we found that 17-AAG rapidly increased Src phosphorylation on Tyr-418, an indicator of Src activation. This phenomenon was seen whether or not the cells were first exposed (for 5 days) to RANKL and M-CSF to promote differentiation into mature osteoclasts (26). Src activation reached a peak at 15 min and subsequently declined, rapidly going below basal level [Fig. 1*A*; also see supporting information (SI) Fig. S1*A*]. There was no discernible change in total Src protein over the 24-h time period

Author contributions: L.N. designed research; A.Y., S.T., S.S., and M.-J.L. performed research; S.S., M.-J.L., J.T., and H.O. contributed new reagents/analytic tools; A.Y., J.T., and L.N. analyzed data; and A.Y. and L.N. wrote the paper.

The authors declare no conflict of interest.

This article is a PNAS Direct Submission.

†Present address: Kyowa Hakko Kirin, Fuji Research Park, Shizuoka, 411-8731 Japan.

¶To whom correspondence should be addressed. E-mail: neckersl@mail.nih.gov.

This article contains supporting information online at www.pnas.org/cgi/content/full/0805354105/DCSupplemental.

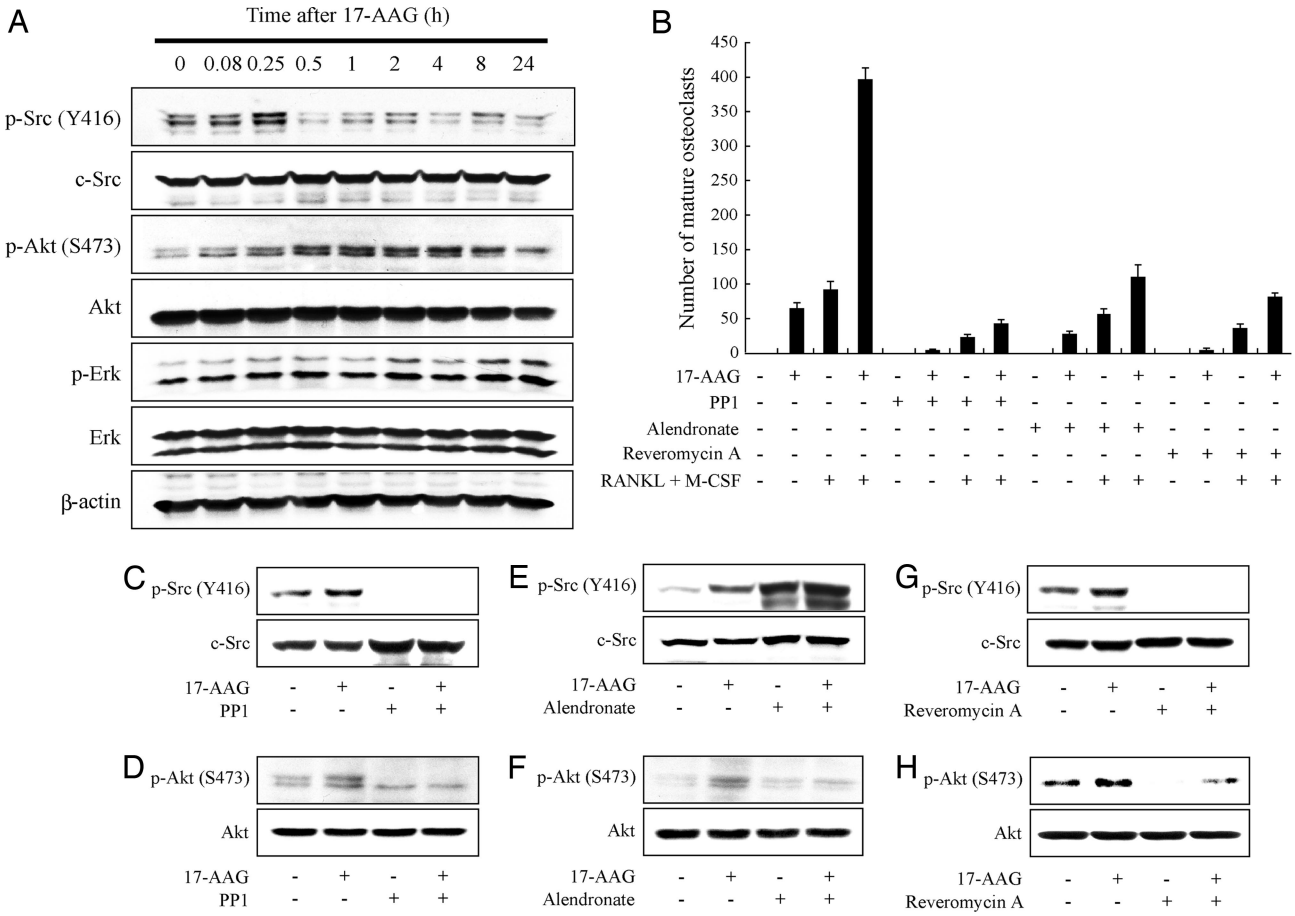

Fig. 1. 17-AAG-induced osteoclastogenesis requires Src kinase activation. (*A*) 17-AAG induces transient phosphorylation of c-Src on Y418 and of Akt on Ser-473. RAW264.7 cells were treated with 1 μM 17-AAG for the indicated times after incubation with 100 ng/ml RANKL and 10 ng/ml M-CSF for 5 days. Phosphorylation and protein levels of Src, Akt, and Erk in total cell lysate were detected by Western blot using specific antibodies. (*B*) 17-AAG induces osteoclastogenesis, which was abolished by either 10 μM PP1, 30 μM alendronate or 5 μM reveromycin A. RAW264.7 cells were treated with 1 μM 17-AAG and indicated reagents in the presence or absence of 100 ng/ml RANKL and 10 ng/ml M-SCF for 5 days. The number of mature osteoclasts with more than three nuclei stained by TRAP was counted. Data are indicated as the mean of three independent experiments ± SEM. (*C–H*) RAW264.7 cells were pretreated with either PP1, alendronate or reveromycin A for 1h and incubated with 1 μM 17-AAG or DMSO for 15 min after incubation with 100 ng/ml RANKL and 10 ng/ml M-SCF for 5 days. Phosphorylation and protein levels were detected as described above.

of the experiment. Akt, also a contributor to osteoclast survival and differentiation (27), was activated as well (*p*-Akt), but its activation peaked later and was more prolonged than that of Src (for at least 8 h; Fig. 1*A*). Erk activation changed minimally during the experiment. As in other cell systems, the Hsp90 client proteins Akt and Raf-1 were both ultimately destabilized by 17-AAG, but this required extended exposure of cells to higher drug concentrations (see Fig. S1*B*). The latency of Akt activation compared to activation of Src suggests that the former could be Src-dependent, as we previously reported in bladder and breast cancer cells (8). That the Src inhibitor PP1 fully blocked 17-AAG-induced Akt activation (Fig. 1*D*) supports this hypothesis.

To examine whether 17-AAG-induced Src activation impacted osteoclastogenesis, we compared the degree of osteoclast maturation under several treatment conditions (Fig. 1*B*). 17-AAG alone increased the number of mature osteoclasts as effectively as did exposure to the cytokines RANKL and M-CSF, whereas a combination of all three treatments was markedly synergistic. Underlining the importance of Src in this process, the Src kinase inhibitor PP1 potently inhibited osteoclast maturation caused by either 17-AAG, RANKL + M-CSF, or the combination of the three agents. Similar inhibitory effects were obtained by treatment with two additional and mechanistically distinct inhibitors of osteoclast bone resorption, alendronate, and reveromycin A. Although reveromycin A, like PP1, blocked 17-AAG-induced Src activation (Fig. 1*G*), alendronate actually promoted even greater Src activation than did 17-AAG (Fig. 1*E*). However, all three inhibitors completely abrogated 17-AAG-induced Akt activation downstream of Src (Fig. 1 *D*, *F*, and *H*), suggesting that Src activation is necessary, but in the absence of Akt activation is not sufficient for osteoclastogenesis to occur.

17-AAG Prolongs M-CSF-Induced Src Kinase Activation and Potentiates Association of Src with c-Fms. The M-CSF receptor, c-Fms, is highly expressed on mature osteoclasts (28), and interaction of M-CSF with c-Fms promotes actin reorganization and cell spreading. Src is likely to be required in this pathway because the ability of M-CSF to modulate cytoskeleton reorganization is not observed in osteoclasts derived from $src^{-/-}$ mice, and M-CSF induces Src-dependent tyrosine phosphorylation in osteoclasts (29, 30). To investigate the possible impact of 17-AAG on this signaling pathway, we first examined the effect of 17-AAG on M-CSF-induced Src activation. Combined treatment with 17-AAG and M-CSF induced a more robust and more prolonged activation of Src compared to treatment with M-CSF alone (Fig. 2 *A–C*). Further, a neutralizing antibody against M-CSF blocked 17-AAG-induced Src phosphorylation (Fig. 2*D*). Finally, 17-AAG increased association of c-Fms with Src (Fig. 2*E*). Taken

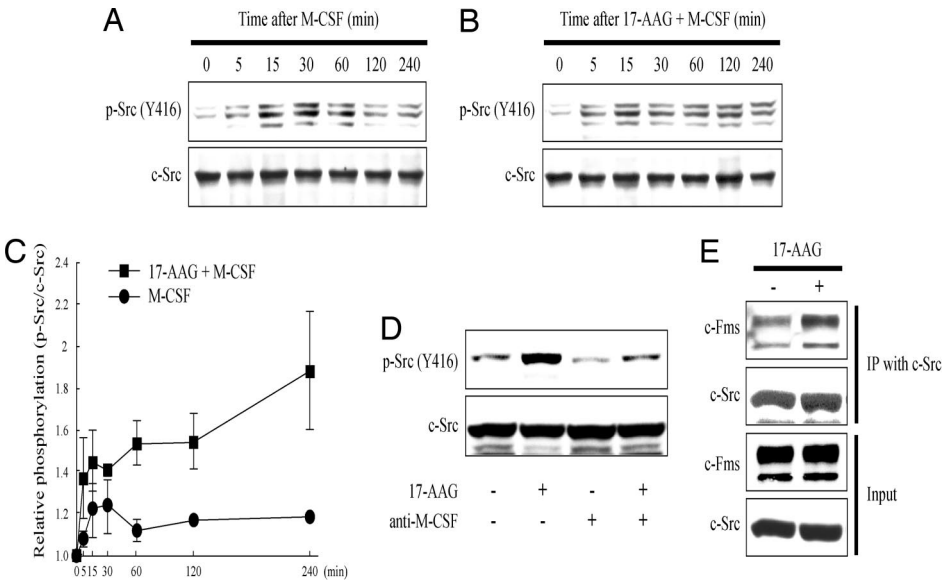

Fig. 2. 17-AAG prolongs M-CSF-induced Src kinase activation and enhances interaction of Src with c-Fms. RAW264.7 cells were incubated with 100 ng/ml RANKL and 10 ng/ml M-CSF for 5 days before treatments described below. (*A*) M-CSF transiently increases phosphorylation of Src Y416. RAW264.7 cells were treated with 100 ng/ml M-CSF for the indicated times. Phosphorylation and protein level of Src in total cell lysate were detected by Western blot. (*B*) 17-AAG increases and prolongs M-CSF-induced Src phosphorylation. RAW264.7 cells were treated with 100 ng/ml M-CSF and 1 μM 17-AAG for the indicated times. Phosphorylation and protein level were detected as described above. (*C*) Relative ratios of phosphorylated Src Y416 to total Src are graphically depicted as a function of time after 1 μM 17-AAG. Data are displayed as the mean of three independent experiments $\pm$ SEM. (*D*) 17-AAG-induced Src kinase activation is abolished by blocking M–CSF function. RAW264.7 cells were pretreated with 20 μg/ml anti-M-CSF antibody for 1 h and incubated with 1 μM 17-AAG or DMSO for 15 min. Phosphorylation and protein level were detected as described above. (*E*) 17-AAG increases the binding of Src to c-Fms. Src was immunoprecipitated from RAW264.7 cells treated as shown with 1 μM 17-AAG for 30 min, and the blot was probed with indicated antibodies.

together, these results suggest that 17-AAG-induced Src activation at least partly depends on the M-CSF/c-Fms signaling pathway and that 17-AAG enhances and prolongs M-CSF-dependent Src activation by promoting Src association with c-Fms.

17-AAG Induces Src-Dependent Phosphorylation of Integrin β3. To further clarify the importance of 17-AAG-induced Src activation in the process of osteoclast maturation, we examined whether 17-AAG promotes phosphorylation of integrin β3, a known Src substrate that, upon phosphorylation, plays an important role in one of the final steps of osteoclastogenesis, cell fusion and spreading, which requires reorganization of the actin cytoskeleton (31–33). We readily detected 17-AAG-induced integrin β3 phosphorylation, which was abrogated by the Src kinase inhibitor PP1 (Fig. 3*A*). As with c-Fms, 17-AAG potentiated the interaction of integrin β3 with Src (Fig. 3*B*).

17-AAG Potentiates Intratibial Growth of Prostate Cancer Cells. Finally, given these observations, we examined whether 17-AAG accelerates *in vivo* prostate cancer growth in bone secondary to its potentiation of osteoclastogenesis as seen in our *in vitro* experiments. Using an intratibial xenograft model of PC-3M luciferase-expressing (PC-3M-luc) cells, we observed that systemically administered 17-AAG significantly increased tumor growth in bone compared to vehicle-treated controls (Fig. 4). These data are in distinct contrast to the inhibitory effects of systemic 17-AAG on PC-3M-luc tumors growing as s.c. xenografts. In this setting, the same dose and schedule of 17-AAG reduced tumor growth by 83% (see Fig. S2), suggesting that drug effects on intraosseous tumor growth are indirect and are likely mediated by the unique cellular environment. To address this possibility, we examined whether any of the three functionally distinct inhibitors of 17-AAG-stimulated osteoclastogenesis that we identified *in vitro* demonstrated any ability to blunt the stimulatory effect of 17-AAG on *in vivo* prostate tumor growth in bone. We observed that each of the three inhibitors was able to at least partially abrogate the *in vivo* tumor-stimulatory effect of 17-AAG (Fig. 4), suggesting that drug-induced activation of Src and Akt in osteoclasts is likely responsible for 17-AAG-dependent tumor growth stimulation in this unique environment.

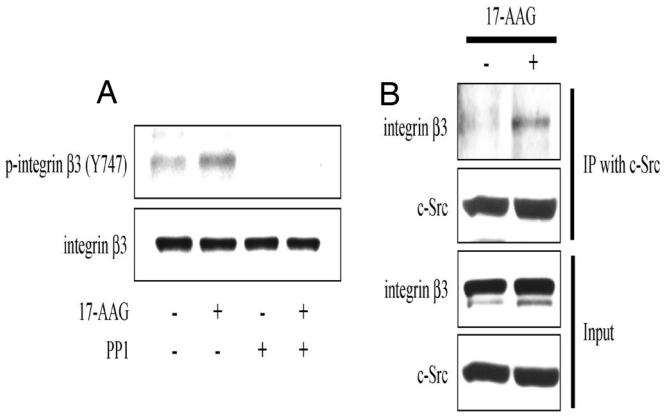

Fig. 3. 17-AAG induces phosphorylation of integrin β3 and promotes association with Src. RAW264.7 cells were incubated with 100 ng/ml RANKL and 10 ng/ml M-CSF for 5 days before treatment as described below. (*A*) RAW264.7 cells were pretreated with 10 μM PP1 for 1 h and incubated with 1 μM 17-AAG or DMSO for 15 min. Phosphorylation and protein level of integrin β3 were determined by Western blot by using total cell lysates. (*B*) 17-AAG potentiates the binding of Src to integrin β3. Src was immunoprecipitated from RAW264.7 cells treated with 1 μM 17-AAG for 30 min, and the blot was probed with indicated antibodies.

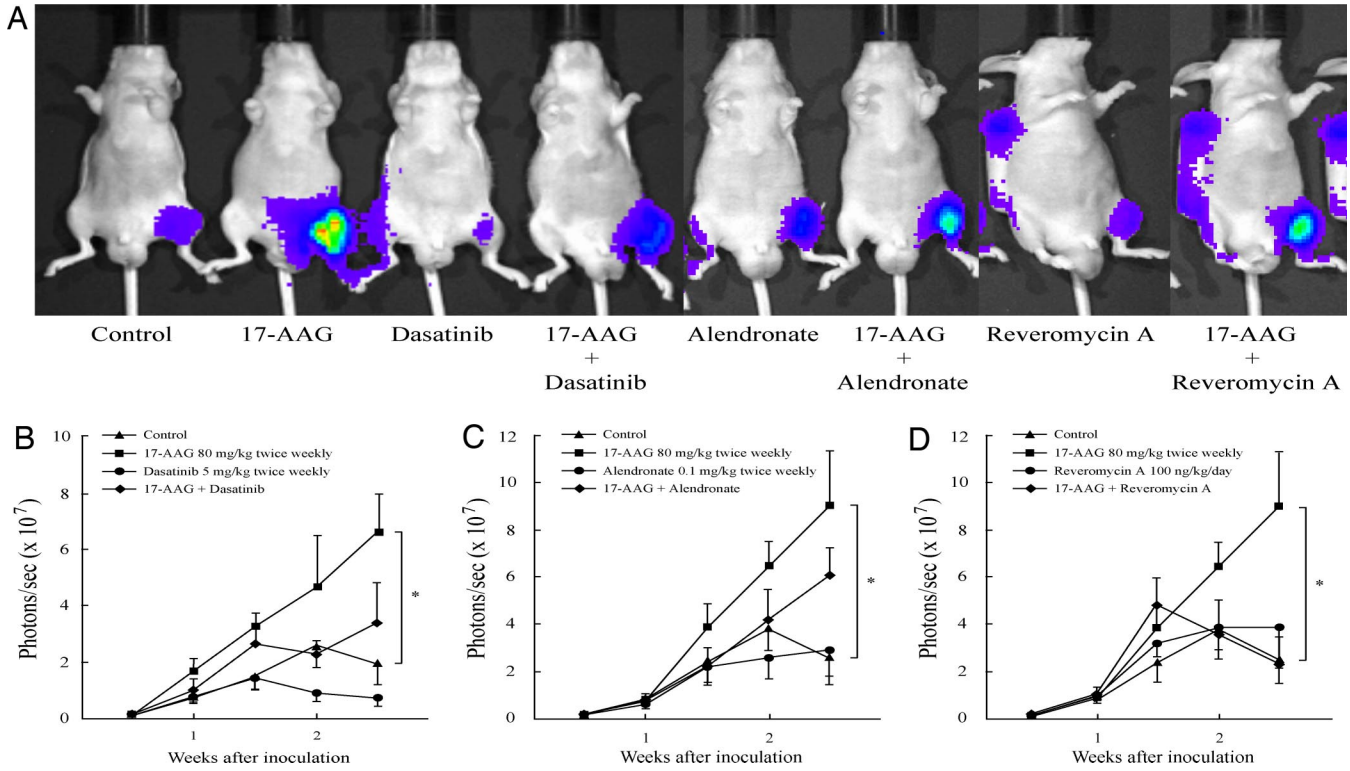

Fig. 4. 17-AAG accelerates *in vivo* tumor growth of prostate cancer cells in bone and this is abrogated by mechanistically distinct inhibitors of osteoclast-mediated bone resorption. (*A*) Typical tumor signal intensity in mice 2.5 weeks after intratibial inoculation. The effect of (*B*) dasatinib (Src inhibitor), (*C*) alendronate (bisphosphonate), and (*D*) reveromycin A on 17-AAG-induced PC-3M-luc growth in bone is graphically displayed. The control group was treated with DMSO i.p. twice weekly. Luciferase activity was detected and quantified by using a bioluminescent IVIS Imaging System. Data are expressed as means ± SEM. *, $P < 0.05$ vs. control.

Discussion

In this study, we have shown that 17-AAG promotes osteoclastogenesis *in vitro* by transiently stimulating a signaling cascade beginning with Src kinase and proceeding to Akt, and that this process can be reversed by a Src inhibitor, a bisphosphonate, or the osteoclast-specific apoptosis inducer reveromycin A. Hsp90-directed therapy inhibited the growth of s.c. PC-3M prostate carcinoma xenografts, but stimulated growth of PC-3M in bone. Each of the three inhibitors of osteoclastogenesis counteracted this activity. These data support and extend the results of a recent report in which 17-AAG was found to promote differentiation of preosteoclasts and to increase bone metastases in a murine breast cancer model (18).

Prostate cancer is the second leading cause of cancer-related death in men in the United States (34) and is known to have a high potential to metastasize to bone. Despite the overall osteoblastic nature of prostate cancer bone metastases, a number of studies suggest that the up-regulation of osteolytic bone resorption also occurs and is essential for initiation of bone metastases (35, 36). Multiple signaling pathways regulate osteoclastogenesis (19), but Src is known to be one of the key components of this process. $Src^{-/-}$ mice show only one major phenotype, osteopetrosis, caused by a functional defect in mature osteoclasts (37, 38). M-CSF is another key regulator of osteoclastogenesis (21, 22), and Src has been implicated in M-CSF signaling through its receptor, c-Fms (29). In the present study, we have shown that M-CSF and 17-AAG cooperate in inducing Src activation. 17-AAG potentiates and prolongs the Src kinase activity induced by M-CSF alone, and a neutralizing antibody to M-CSF blocks 17-AAG-induced Src activation. In the osteoclast maturation program, M-CSF is required for Src-dependent cytoskeletal reorganization, during which Src associates with and phosphorylates integrin $\beta 3$ (30, 33). Here, we demonstrate that 17-AAG and M-CSF synergistically activate Src-mediated integrin $\beta 3$ phosphorylation (31, 33).

Although 17-AAG-stimulated signaling cascades and osteoclastogenesis can be abrogated *in vitro* by a Src inhibitor, a bisphosphonate, or reveromycin A, treatment with alendronate increased Src kinase activation whereas decreasing Akt activation, which our current and previous (8) data suggest is downstream of Src. Nitrogen-containing bisphosphonates such as alendronate are known to prevent prenylation of small GTPases, which play an important role in osteoclast actin reorganization downstream of Src (38). Therefore, alendronate-induced Src activation could be the net result of negative feedback following disruption of this signaling pathway.

It is important to note that not all tumors growing in bone appear to be similarly affected by 17-AAG. Mitsiades *et al.* (6) reported recently that 17-AAG is efficacious in preventing lytic bone lesions associated with multiple myeloma. This observation, combined with high antimyeloma activity of 17-AAG, led to initiation of a phase III trial of 17-AAG in this disease (ClinicalTrials.gov identifier: NCT00546780). These investigators examined GFP-expressing tumor cells for their *in vivo* analyses, and they did not specifically examine bone density after treatment with 17-AAG. Because multiple myeloma is highly sensitive to Hsp90 inhibition, it is possible that tumor killing by the drug took precedence over any effects on the local bone environment. It would be informative to determine bone density in these mice at the conclusion of 17-AAG treatment. Alternatively, Mitsiades *et al.* (6) used SCID/NOD mice for their *in vivo* experiments, whereas we used NCr Nu/Nu mice, and Price *et al.* (18) used BALB/c Nu/Nu and C57BL/6 mice. Thus, mouse strain differences in osteoclast number and/or response to 17-AAG

cannot be ruled out at this time. Nonetheless, a conservative interpretation of these findings suggests that bone density and intraosseous metastases should be monitored in patients receiving Hsp90 inhibitors. If it is proven to be necessary to counter the osteoclastogenic activity of 17-AAG or other Hsp90 inhibitors, our results suggest that co-administration of either a Src inhibitor or other antagonist of osteoclast-mediated bone resorption may be considered.

Finally, this study emphasizes an important consideration that has received less attention than perhaps is warranted, namely the possible long-term impact of Hsp90 inhibitors on normal tissues. To date, most efforts have been focused on identifying the potential dose-limiting and most likely off-target toxicities of these drugs. As improved, chemically less reactive, and less toxic Hsp90 inhibitors reach the clinic, the likelihood of prolonged *in vivo* exposure to these drugs will increase, as will the possibility that signaling pathways in normal tissues may be affected in unpredictable ways. Besides having a possible impact on homeostatic processes of normal tissue, such as regulation of bone density, indirect and unintended effects on localized tumor growth may also occur.

Tyrosine kinase-addicted tumors escape molecularly targeted inhibitors by mutations that interfere with drug binding (e.g., mutations in the kinase domain of Bcr-Abl and EGFR) or by a process termed "oncogene switching," whereby drug-treated cells use an alternative tyrosine kinase to drive downstream signaling pathways (e.g., c-Met or IGF-1 receptor utilization nonsmall cell lung cancers exposed to EGFR tyrosine kinase inhibitors) (39–42). It has been proposed that cancer cells by their very nature may be "Hsp90 addicted" (43), yet neither drug-sparing mutations nor utilization of alternative chaperones have been identified in Hsp90 inhibitor-treated tumor cells to date. Although encouraging, these observations do not address the possibility that tumor environment may indirectly impact drug efficacy. For example, stromal-mediated protection of leukemia cells in bone marrow from the anticancer activity of tyrosine kinase inhibitors has been reported recently (44, 45). Likewise, our data identify Hsp90-dependent, osteoclast-mediated protection of certain solid tumors from Hsp90 inhibitors as a potentially important mechanism of chemoresistance that must be overcome to achieve the optimal clinical benefit of these highly promising molecularly targeted drugs.

Materials and Methods

Cell Culture and Reagents. RAW 264.7 cells (American Type Culture Collection) and PC-3M-luc cells were maintained in MEM (α modification) and RPMI medium 1640, respectively, containing 10% FBS, 2 mM L-glutamine, 100 units/ml penicillin, and 100 μg/ml streptomycin at 37°C and 5% CO_2. For osteoclastogenesis experiments, RAW cells were cultured for 5 days in a six-well tissue culture plate in the presence of 100 ng/ml RANKL (PeproTech) and 10 ng/ml M-CSF (R&D Systems) (26). For immunoblotting, antibodies to phospho-Ser-473 Akt, Akt, phospho-Tyr-416 Src, c-Src, phsopho-Erk1/2 (clone 10), Erk1/2 (Cell Signaling Technology), phospho-Tyr-747 integrin β3 (Santa Cruz Biotechnology), integrin β3 (Chemicon International), and c-Fms (Santa Cruz Biotechnology) were used. 17-AAG was obtained from Kosan Biosciences. PP1 and anti-mouse M-CSF neutralizing antibody were purchased from BIOMOL International and R&D Systems, respectively. Dasatinib (46) was obtained from Bristol Myers Squibb.

TRAP Staining. A TRAP staining kit (Sigma) was used to quantify mature osteoclasts. Briefly, cells were fixed with 10% buffered formalin for 2 min. After rinsing in deionized water, cells were put into TRAP staining solution for 1 h according to the manufacturer's protocol.

Immunoprecipitation and Immunoblotting. These experiments were performed as described (47). Briefly, cells were lysed by scraping in lysis buffer [20 mM Tris·HCl (pH 7.5), 150 mM NaCl, 1 mM EDTA, 1% Triton X-100, 50 mM NaF, 2 mM Na_3VO_4] supplemented with Complete proteinase inhibitors (Roche). For immunoprecipitation, TNMSV lysis buffer [50 mM Tris·HCl (pH 7.4), 0.1% Nonidet P-40, 20 mM Na_2MoO_4, 150 mM NaCl, 2 mM Na_3VO_4] was used. Immunoprecipitates or cell lysate were resolved by 7.5% or 4–20% SDS/PAGE, transferred to nitrocellulose membrane, and probed with respective antibodies.

Quantitative Analysis of Prostate Cancer Cells in Bone. Animal experiments and procedures were carried out in accordance with the Guide for the Care and Use of Laboratory Animals as adopted and promulgated by the National Institutes of Health. To establish a PC-3M luciferase-expressing (PC-3M-luc) tumor xenograft model, PC-3M-luc cells growing *in vitro* were detached with trypsin, and mixed with RPMI medium 1640 (without FBS) immediately before inoculation. Cells (1×10^6) were injected into the tibia of male Nu/Nu mice (6 weeks of age, Taconic). After the first evaluation of tumor signal intensity by bioluminescent imaging using an IVIS Imaging System (Xenogen), mice were randomly assigned to treatment groups (six to eight mice each). Each mouse was given drugs by i.p. (17-AAG and dasatinib) or s.c. (alendronate) injection twice weekly, except for reveromycin A, which was administered by s.c. implanted miniosmotic pump to allow for continuous delivery (Alzet model 2004). Drug dosages were: 17-AAG, 80 mg/kg; dasatinib, 5 mg/kg; alendronate, 0.1 mg/kg; reveromycin A, 100 μg/kg/day.

Statistical Analysis. For multiple comparisons, the significant difference was analyzed using one-way ANOVA followed by a multiple comparison Dunnett's test. Data represent the mean $\pm$ SEM. All P values <0.05 were considered statistically significant. All statistical tests were two sided. Statistical analysis was done with JMP 5.0 software (SAS Institute).

ACKNOWLEDGMENTS. Grant support was provided by funds from the Intramural Research Program of the National Institutes of Health, National Cancer Institute.

1. Neckers L (2002) Hsp90 inhibitors as novel cancer chemotherapeutic agents. *Trends Mol Med* 8:S55–S61.
2. Whitesell L, Lindquist SL (2005) HSP90 and the chaperoning of cancer. *Nat Rev Cancer* 5:761–772.
3. Workman P, Burrows F, Neckers L, Rosen N (2007) Drugging the cancer chaperone HSP90: Combinatorial therapeutic exploitation of oncogene addiction and tumor stress. *Ann NY Acad Sci* 1113:202–216.
4. Solit DB, *et al.* (2002) 17-Allylamino-17-demethoxygeldanamycin induces the degradation of androgen receptor and HER-2/neu and inhibits the growth of prostate cancer xenografts. *Clin Cancer Res* 8:986–993.
5. Bisht KS, *et al.* (2003) Geldanamycin and 17-allylamino-17-demethoxygeldanamycin potentiate the in vitro and in vivo radiation response of cervical tumor cells via the heat shock protein 90-mediated intracellular signaling and cytotoxicity. *Cancer Res* 63:8984–8995.
6. Mitsiades CS, *et al.* (2006) Antimyeloma activity of heat shock protein-90 inhibition. *Blood* 107:1092–1100.
7. Modi S, *et al.* (2007) Combination of trastuzumab and tanespimycin (17-AAG, *KOS-953*) is safe and active in trastuzumab-refractory HER-2 overexpressing breast cancer: A phase I dose-escalation study. *J Clin Oncol* 25:5410–5417.
8. Koga F, *et al.* (2006) Hsp90 inhibition transiently activates Src kinase and promotes Src-dependent Akt and Erk activation. *Proc Natl Acad Sci USA* 103:11318–11322.
9. Donze O, Abbas-Terki T, Picard D (2001) The Hsp90 chaperone complex is both a facilitator and a repressor of the dsRNA-dependent kinase PKR. *EMBO J* 20:3771–3780.
10. Yun BG, Matts RL (2005) Hsp90 functions to balance the phosphorylation state of Akt during C2C12 myoblast differentiation. *Cell Signal* 17:1477–1485.
11. Citri A, *et al.* (2004) Hsp90 restrains ErbB-2/HER2 signalling by limiting heterodimer formation. *EMBO Rep* 5:1165–1170.
12. Lattouf JB, Srinivasan R, Pinto PA, Linehan WM, Neckers L (2006) Mechanisms of disease: the role of heat-shock protein 90 in genitourinary malignancy. *Nat Clin Practice* 3:590–601.
13. Solit DB, Rosen N (2006) Hsp90: A novel target for cancer therapy. *Curr Top Med Chem* 6:1205–1214.
14. Saporita AJ, Ai J, Wang Z (2007) The Hsp90 inhibitor, 17-AAG, prevents the ligand-independent nuclear localization of androgen receptor in refractory prostate cancer cells. *Prostate* 67:509–520.
15. Williams CR, Tabios R, Linehan WM, Neckers L (2007) Intratumor injection of the Hsp90 inhibitor 17AAG decreases tumor growth and induces apoptosis in a prostate cancer xenograft model. *J Urol* 178:1528–1532.
16. Eccles SA, *et al.* (2008) NVP-AUY922: A novel heat shock protein 90 inhibitor active against xenograft tumor growth, angiogenesis, and metastasis. *Cancer Res* 68:2850–2860.
17. Niu G, Cai W, Chen K, Chen X (2008) Non-invasive PET imaging of EGFR degradation induced by a heat shock protein 90 inhibitor. *Mol Imaging Biol* 10:99–106.
18. Price JT, *et al.* (2005) The heat shock protein 90 inhibitor, 17-allylamino-17-demethoxygeldanamycin, enhances osteoclast formation and potentiates bone metastasis of a human breast cancer cell line. *Cancer Res* 65:4929–4938.
19. Boyle WJ, Simonet WS, Lacey DL (2003) Osteoclast differentiation and activation. *Nature* 423:337–342.
20. Miyazaki T, *et al.* (2004) Src kinase activity is essential for osteoclast function. *J Biol Chem* 279:17660–17666.

21. Yoshida H, *et al.* (1990) The murine mutation osteopetrosis is in the coding region of the macrophage colony stimulating factor gene. *Nature* 345:442–444.
22. Dai XM, *et al.* (2002) Targeted disruption of the mouse colony-stimulating factor 1 receptor gene results in osteopetrosis, mononuclear phagocyte deficiency, increased primitive progenitor cell frequencies, and reproductive defects. *Blood* 99:111–120.
23. Boyce BF, *et al.* (2003) Regulation of bone remodeling and emerging breakthrough drugs for osteoporosis and osteolytic bone metastases *Kidney Int*, S2–5.
24. Roelofs AJ, Thompson K, Gordon S, Rogers MJ (2006) Molecular mechanisms of action of bisphosphonates: current status. *Clin Cancer Res* 12:6222s–6230s.
25. Woo JT, *et al.* (2006) Reveromycin A, an agent for osteoporosis, inhibits bone resorption by inducing apoptosis specifically in osteoclasts. *Proc Natl Acad Sci USA* 103:4729–4734.
26. Hotokezaka H, *et al*. (2002) U0126 and PD98059, specific inhibitors of MEK, accelerate differentiation of RAW264.7 cells into osteoclast-like cells. *J Biol Chem* 277:47366–47372.
27. Sugatani T, Hruska KA (2005) Akt1/Akt2 and mammalian target of rapamycin/Bim play critical roles in osteoclast differentiation and survival, respectively, whereas Akt is dispensable for cell survival in isolated osteoclast precursors. *J Biol Chem* 280:3583–3589.
28. Yang M, *et al*. (2006) Chemokine and chemokine receptor expression during colony stimulating factor-1-induced osteoclast differentiation in the toothless osteopetrotic rat: A key role for CCL9 (MIP-1gamma) in osteoclastogenesis *in vivo* and *in vitro*. *Blood* 107:2262–2270.
29. Insogna KL, *et al*. (1997) Colony-stimulating factor-1 induces cytoskeletal reorganization and c-src-dependent tyrosine phosphorylation of selected cellular proteins in rodent osteoclasts. *J Clin Invest* 100:2476–2485.
30. Sakai H, *et al*. (2006) Activated c-Fms recruits Vav and Rac during CSF-1-induced cytoskeletal remodeling and spreading in osteoclasts. *Bone* 39:1290–1301.
31. Boissy P, *et al.* (1998) Aggregation of mononucleated precursors triggers cell surface expression of alphavbeta3 integrin, essential to formation of osteoclast-like multinucleated cells. *J Cell Sci* 111:2563–2574.
32. Datta A, Huber F, Boettiger D (2002) Phosphorylation of beta3 integrin controls ligand binding strength. *J Biol Chem* 277:3943–3949.
33. Ross FP, Teitelbaum SL (2005) alphavbeta3 and macrophage colony-stimulating factor: partners in osteoclast biology. *Immunol Rev* 208:88–105.
34. Jemal A, *et al.* (2008) Cancer statistics, 2008. *CA Cancer J Clin* 58:71–96.
35. Zhang J, *et al.* (2001) Osteoprotegerin inhibits prostate cancer-induced osteoclastogenesis and prevents prostate tumor growth in the bone. *J Clin Invest* 107:1235–1244.
36. Keller ET, Brown J (2004) Prostate cancer bone metastases promote both osteolytic and osteoblastic activity. *J Cell Biochem* 91:718–729.
37. Soriano P, Montgomery C, Geske R, Bradley A (1991) Targeted disruption of the c-src proto-oncogene leads to osteopetrosis in mice. *Cell* 64:693–702.
38. Faccio R, *et al.* (2005) Vav3 regulates osteoclast function and bone mass. *Nat Med* 11:284–290.
39. von Bubnoff N, Peschel C, Duyster J (2003) Resistance of Philadelphia-chromosome positive leukemia towards the kinase inhibitor imatinib (STI571, *Glivec*): *A* targeted oncoprotein strikes back. *Leukemia* 17:829–838.
40. Kobayashi S, *et al.* (2005) EGFR mutation and resistance of non-small-cell lung cancer to gefitinib. *N Engl J Med* 352:786–792.
41. Engelman JA, *et al*. (2007) MET amplification leads to gefitinib resistance in lung cancer by activating ERBB3 signaling. *Science* 316:1039–1043.
42. Morgillo F, *et al.* (2007) Implication of the insulin-like growth factor-IR pathway in the resistance of non-small cell lung cancer cells to treatment with gefitinib. *Clin Cancer Res* 13:2795–2803.
43. Xu W, Neckers L (2007) Targeting the molecular chaperone heat shock protein 90 provides a multifaceted effect on diverse cell signaling pathways of cancer cells. *Clin Cancer Res* 13:1625–1629.
44. Mishra S, Zhang B, Cunnick JM, Heisterkamp N, Groffen J (2006) Resistance to imatinib of bcr/abl p190 lymphoblastic leukemia cells. *Cancer Res* 66:5387–5393.
45. Weisberg E, *et al.* (2008) Stromal-mediated protection of tyrosine kinase inhibitor-treated BCR-ABL-expressing leukemia cells. *Molecular Cancer Ther* 7:1121–1129.
46. Johnson FM, Saigal B, Talpaz M, Donato NJ (2005) Dasatinib (BMS-354825) tyrosine kinase inhibitor suppresses invasion and induces cell cycle arrest and apoptosis of head and neck squamous cell carcinoma and non-small cell lung cancer cells. *Clin Cancer Res* 11:6924–6932.
47. Xu W, *et al*. (2001) Sensitivity of mature Erbb2 to geldanamycin is conferred by its kinase domain and is mediated by the chaperone protein Hsp90 *J Biol Chem* 276:3702–3708.